NUCL SCI TECH (2019) 30:13
https://doi.org/10.1007/s41365-018-0533-7

Theoretical calculation and evaluation of n + ^{240,242,244}Pu reactions

Hai-Rui Guo[1] · Yin-Lu Han[2] · Chong-Hai Cai[3]

Received: 5 June 2018 / Revised: 8 October 2018 / Accepted: 9 October 2018 / Published online: 2 January 2019

Abstract The nuclear data of $n + {}^{240,242,244}$Pu reactions for incident energy below 200 MeV are calculated and evaluated to meet the requirement in the design of an accelerator-driven subcritical system. The optical model is used to calculate the total, nonelastic, shape elastic cross sections, shape elastic scattering angular distributions, and transmission coefficients. The distorted-wave Born approximation is applied to calculate the direct inelastic scatterings to the discrete excited states. The nuclear reaction statistical models and fission theory are applied to describe neutron, proton, deuteron, triton, helium-3, alpha and γ emissions, and fission consistently. The results thus obtained are compared with experimental data and the evaluated data obtained from ENDF/B-VII.1 and JENDL-4.0.

Keywords n + ^{240,242,244}Pu reactions · Theoretical calculation of nuclear reaction · Nuclear data for $E \leq 200$ MeV

This work was supported by the National Natural Science Foundation of China-NSAF (No. U1630122) and IAEA Coordinated Research Projects (CRPs) on Recommended Input Parameter Library (RIPL) for Fission Cross Section Calculations (No. 20464).

✉ Yin-Lu Han
hanyl@ciae.ac.cn

1 Institute of Applied Physics and Computational Mathematics, Beijing 100094, China

2 China Institute of Atomic Energy, Beijing 102413, China

3 Department of Physics, Nankai University, Tianjin 300071, China

1 Introduction

In order to improve the public acceptance of nuclear energy and facilitate the sustainable use of uranium resources, an increasing number of studies on accelerator-driven subcritical systems (ADSs) are being conducted globally. The ADS is a promising approach for burning the uranium, plutonium, and minor actinides in the spent fuel with the fast neutrons to generate energy while transmuting the long-lived radioactive fission products with the high-flux neutrons. The new nuclear energy system places new requirements of high-precision nuclear data of neutron-induced reactions on many related nuclides at incident energies below 200 MeV [1, 2]. Plutonium is an important component of the spent fuel and depletion chain, and thus, accurate nuclear data of neutron-induced reactions on plutonium isotopes are essential for the design of an ADS. In our previous study [3], the theoretical analysis and evaluation of an $n + {}^{239}$Pu reaction were introduced. In this study, we focus on neutron-induced reactions on ^{240}Pu, ^{242}Pu, and ^{244}Pu. In addition, the theoretical study of $n + {}^{240,242,244}$Pu reactions is important for understanding the reaction mechanism of fertile nuclei and their structure.

The evaluation data of $n + {}^{240,242,244}$Pu reactions for an incident energy below 20 MeV are provided in the JENDL-4.0 database [4]. The nuclear data of an $n + {}^{240}$Pu reaction for an incident energy below 30 MeV are given in ENDF/B-VII.1 [5], and the data for the $n + {}^{242,244}$Pu reactions from JENDL-4.0 are adopted in the ENDF/B-VII.1 with a few modifications to the resonance cross sections and (n, γ) cross section for the $n + {}^{242}$Pu reaction. The data regarding light-charged-particle (proton, deuteron, triton, helium-3, and alpha) emission are not available in ENDF/B-VII.1 and

JENDL-4.0. For meeting the ADS design requirements, the energy maximum of the nuclear data is required to be extended to 200 MeV. Subsequent to the evaluations for ENDF/B-VII.1 and JENDL-4.0, some new experimental data have been provided; in particular, some fission and capture cross sections were measured at the Los Alamos Neutron Science Center (LANSCE) using world-class advanced experimental facilities in recent years. These new experimental data are also required to be considered in the new evaluation.

Experimental data for $n+{}^{240,242,244}Pu$ reactions are lacking, and there exist some discrepancies among the experimental data from various groups. Thus, self-consistent calculation of each reaction using theoretical models is important. In this work, all cross sections, angular distributions, energy-angle distributions of neutron and light-charged-particle emissions, number of neutrons per fission, and prompt fission neutron spectra are calculated for an incident energy below 200 MeV. The optical model, distorted-wave Born approximation (DWBA), preequilibrium and equilibrium emission theories, fission model, intranuclear cascade model, and recent experimental data are used. The calculated results are analyzed and compared with the experimental data and the evaluation data obtained from ENDF/B-VII.1 and JENDL-4.0.

In Sect. 2, the theoretical models are briefly outlined, and in Sect. 3, the present results are compared with the experimental data and analyzed. Finally, a summary is presented in Sect. 4.

2 Theoretical model

The optical model is the basis of nuclear reaction analyses. Here, the phenomenological global optical model potential (GOP) from Ref. [6], which has a good prediction power for nucleon-actinide reactions, is adopted to describe the interactions between a neutron and ${}^{240,242,244}Pu$. The total, nonelastic, elastic cross sections, and elastic scattering angular distributions are calculated using the GOP. The DWBA is applied to obtain the direct inelastic scatterings to the discrete levels of ${}^{240,242,244}Pu$. The experimental data of the inelastic cross sections and angular distributions are used to guide the theoretical calculation. The GOP obtained from Ref. [6] is also applied in the DWBA calculation. The corresponding calculation code applied is DWUCK4 [7].

The equilibrium and preequilibrium emission processes at incident energies below 20 MeV are analyzed using the unified Hauser–Feshbach and exciton model [8]. The Hauser–Feshbach theory with width fluctuation correction describes the compound-nucleus decay. The angular-momentum-dependent exciton model, which takes into consideration the parity and angular-momentum conservations, describes the preequilibrium emission process. The summation of the occupation probabilities of preequilibrium and equilibrium states is 1. The multi-step Hauser–Feshbach model is used to calculate secondary particle emissions. The back-shifted Fermi gas level densities [9] are applied to describe the continuum states of compound nuclei. The recoil effect is considered in all reaction

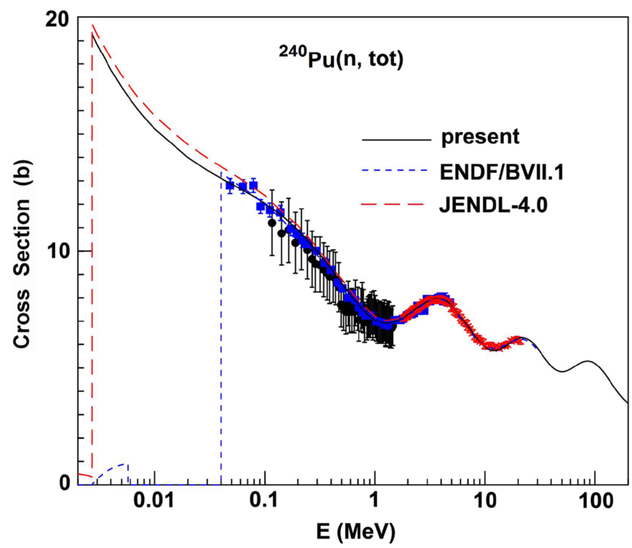

Fig. 1 (Color online) Calculated total cross section (solid line) for the $n+{}^{240}Pu$ reaction as compared with the experimental data (solid circles [27], solid squares [28], and crosses [29]) and the evaluated data obtained from ENDF/B-VII.1 (short-dashed line) and JENDL-4.0 (dashed line)

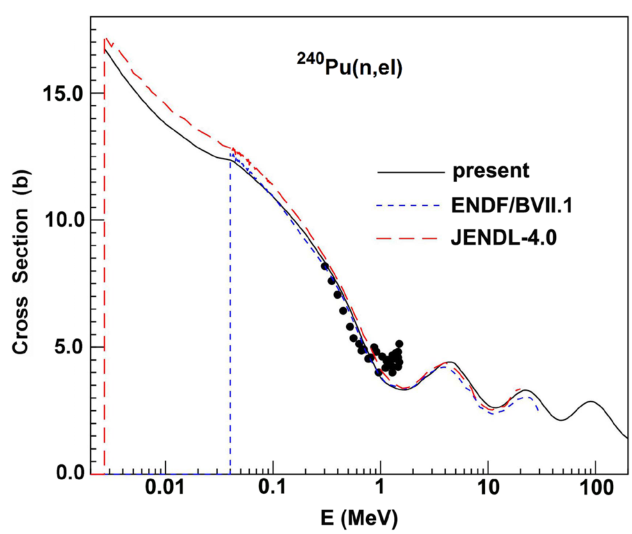

Fig. 2 (Color online) Same as Fig. 1, but for neutron elastic scattering cross section

processes. The energy-angle distributions of emitted particles are calculated using the angular-momentum-dependent exciton state lifetimes, which are obtained by solving the generalized master equation. The improved Iwamoto–Harada pickup mechanism [10, 11] is used in the description of the complex particle (d, t, ^{3}He, α) emissions.

The preequilibrium and equilibrium particle emission in the incident energy region above 20 MeV are calculated using the intranuclear cascade model, exciton model, evaporation model, and Hauser–Feshbach theory with width fluctuation correction. The 1st to the 18th particle emissions from equilibrium states are analyzed using the Hauser–Feshbach theory with the width fluctuation correction and evaporation model. Ignatyuk's description of nuclear level densities [12] is applied to describe the continuum states of compound nuclei. The first to the fifth particle emissions in the preequilibrium reactions are analyzed using the exciton model, and the cascade emissions of one to four nucleons are calculated using the empirical formula presented in Ref. [13]. The energy-angle distributions of emitted particles at incident energies

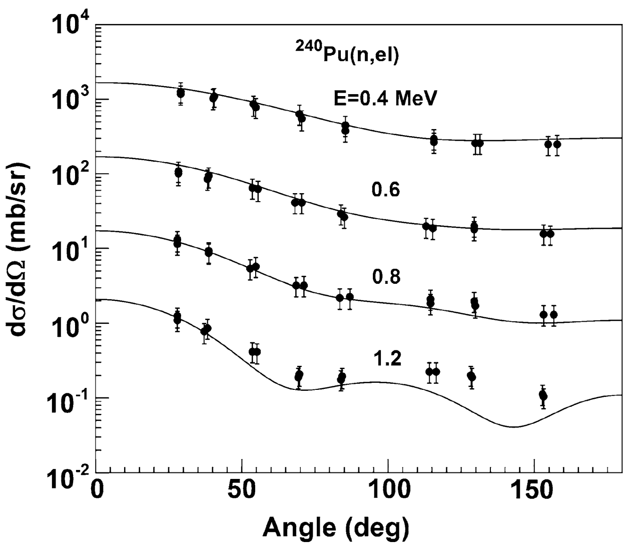

Fig. 3 Elastic scattering angular distribution for n + ^{240}Pu reaction. The data are shifted downward by factors of 10^0, 10^{-1}, 10^{-2} and 10^{-3}

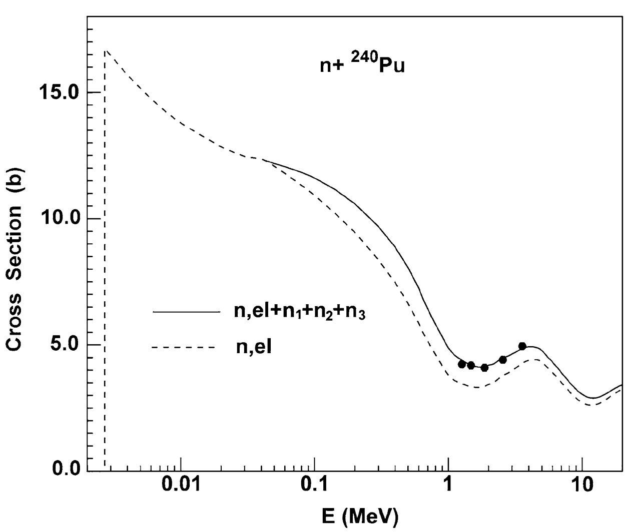

Fig. 4 Cross sections of neutron elastic and inelastic scatterings to the first, second, and third excited levels of ^{240}Pu. The dashed line indicates the calculated elastic scattering cross section, while the solid line and circles denote the calculated result and experimental data of the total contribution from the elastic channel and the three inelastic scattering channels, respectively

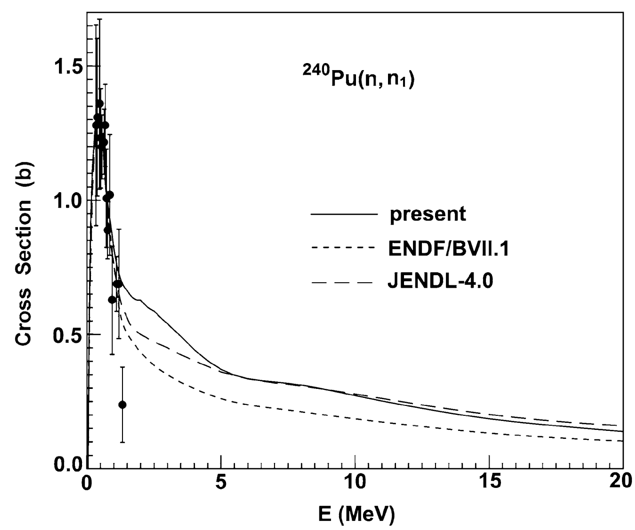

Fig. 5 Calculated cross section (solid line) of neutron inelastic scattering to the first excited level of ^{240}Pu as compared with the experimental (symbols), ENDF/B-VII.1 (short-dashed line), and JENDL-4.0 (dashed line) data

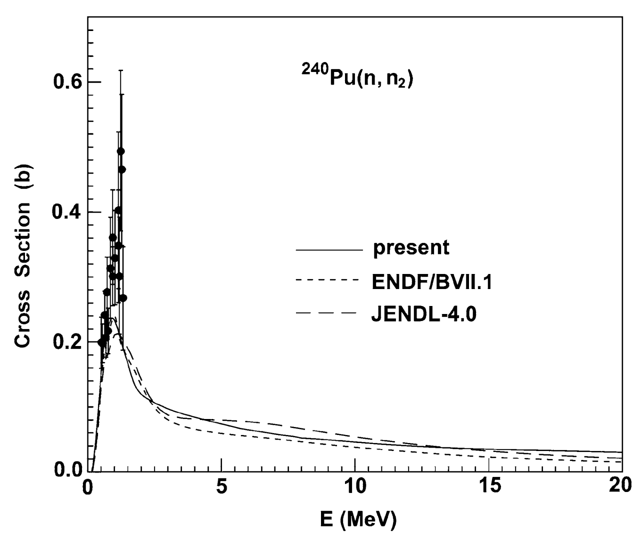

Fig. 6 Same as Fig. 5, but for neutron inelastic scattering to the second excited level of ^{240}Pu

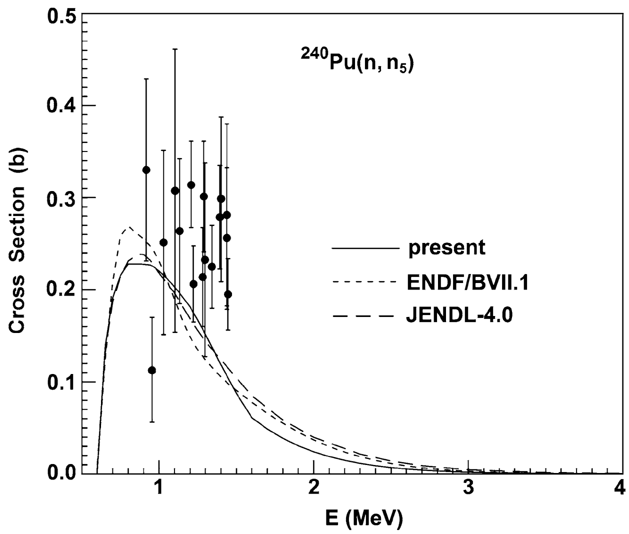

Fig. 7 Same as Fig. 5, but for neutron inelastic scattering to the fifth excited level of ^{240}Pu

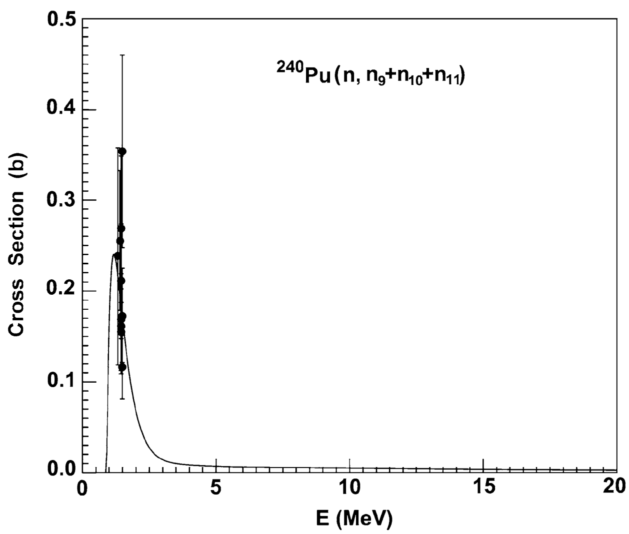

Fig. 8 Same as Fig. 5, but for neutron inelastic scatterings to the 9th, 10th, and 11th excited states of ^{240}Pu

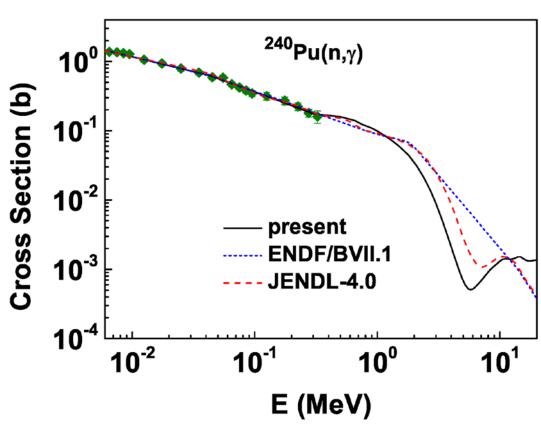

Fig. 9 (Color online) Same as Fig. 1, but for (n, γ) cross section

greater than 20 MeV are obtained by using the Kalbach systematics [14, 15]. The energy-dependent improved Iwamoto–Harada pickup mechanism is also used in this energy region above 20 MeV to describe the composite particle emissions. The UNF code [16] and MEND code [17] are applied below and above 20 MeV, respectively, as in Ref. [18].

The optical model potentials for a nucleon [6], deuteron [19], triton [20], helium-3 [21], and alpha [22] are used to calculate inverse cross sections and transmission coefficients.

Fission is considered as a compound-nucleus decay channel. Uncoupled fission barriers are used to describe

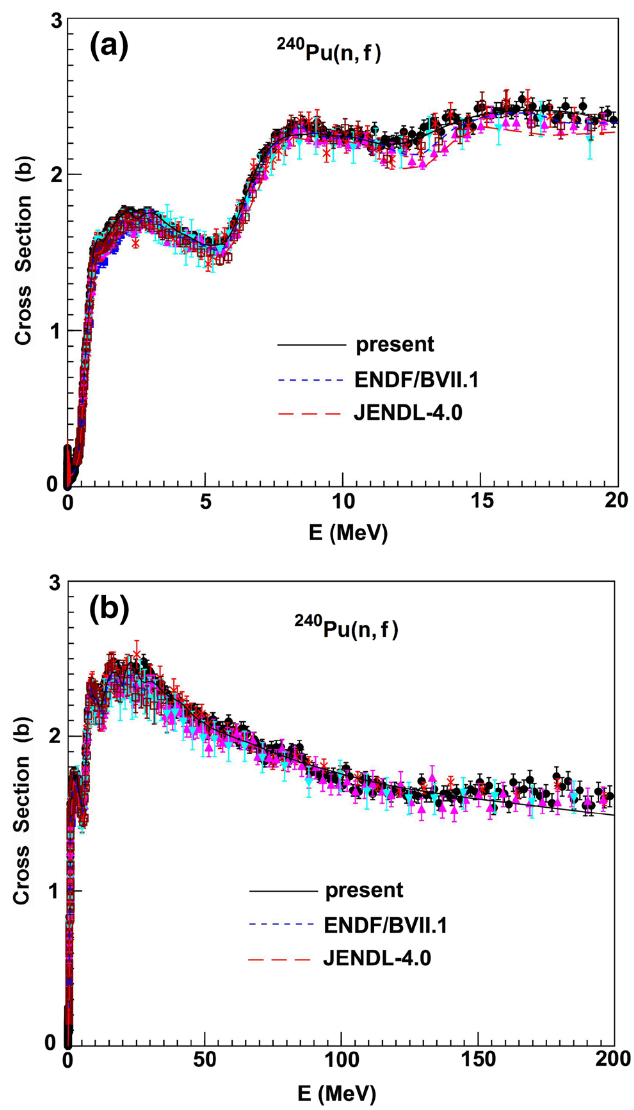

Fig. 10 (Color online) Calculated fission cross section (solid lines) for n + ^{240}Pu reaction as compared with the experimental data (solid circles [32], crosses [33], lower triangles [34], squares [35], upper triangles [36]), and ENDF/B-VII.1 (short-dashed lines) and JENDL-4.0 (dashed lines) data. **a** Incident energies less than 20 MeV and **b** incident energies less than 200 MeV

(n,f), (n,nf), (n,2nf), ..., (n,15nf) fissions. There are a series of transition states characterized by the excited energy above the barrier, spin, and parity at each barrier. The continuum transition states are described by the Gilbert–Cameron level density [23]. The Bohr–Wheeler theory [24, 25] is used to calculate the fission rate. The height and curvature parameters of the fission barriers, level density parameters, and pair corrections at saddle points are obtained by fitting the experimental data. The fission spectra are calculated using the Madland–Nix formula [26].

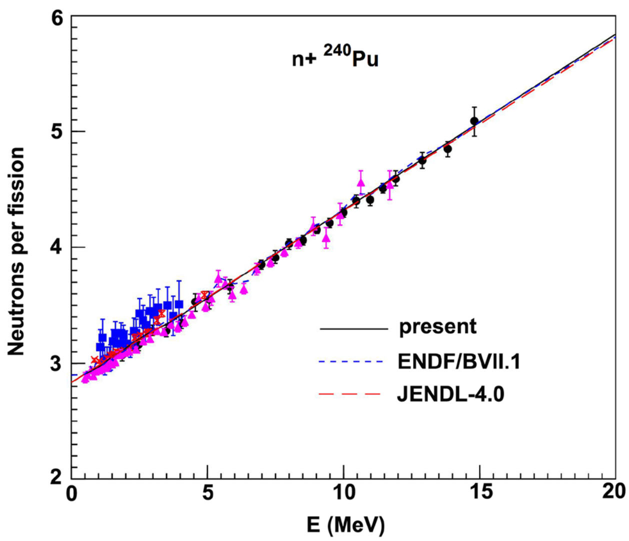

Fig. 11 (Color online) Calculated result of the number of neutrons per fission (solid line) for $n + {}^{240}Pu$ reaction as compared with the experimental (symbols), ENDF/B-VII.1 (short-dashed line), and JENDL-4.0 (dashed line) data

3 Results and analysis

3.1 $n + {}^{240}Pu$ reaction

The calculated total cross section of the $n + {}^{240}Pu$ reaction is compared with experimental data [27–29] and evaluated data obtained from ENDF/B-VII.1 and JENDL-4.0 in Fig. 1. The obtained result reproduces the experimental data rather well and has a slight discrepancy with the ENDF/B-VII.1 and JENDL-4.0 data. It should be noted that all the resonance cross sections in this work are obtained from JENDL-4.0 and are not plotted in the figures. Each curve reduces to 0 at the upper limit of the resonance energy region.

A set of consistent experimental data [27] of the cross section and angular distribution of neutron elastic scattering from ${}^{240}Pu$ was presented by Smith et al. in 1972. The calculated elastic scattering cross section is in good agreement with the experimental data for an incident energy of less than 1 MeV but is less than that of the experimental data for an incident energy between 1 and 2 MeV, as shown in Fig. 2. Similarly, the calculated result of the elastic scattering angular distribution is in good agreement with the experimental data for an incident energy less than 0.8 MeV but is less than that of the experimental data for back angles for an incident energy of 1.2 MeV, as shown in Fig. 3. Another set of experimental data [30] regarding the scattering cross section contributed by the neutron elastic scattering and inelastic scatterings to the first, second, and third excited states of ${}^{240}Pu$ was presented by Smith et al. in 1982. The calculated result reproduces the later experimental data well in the incident

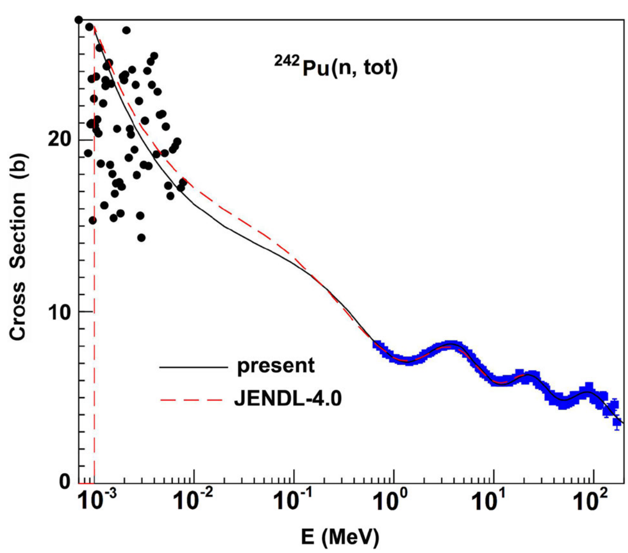

Fig. 12 (Color online) Calculated total cross section (solid line) for $n + {}^{242}Pu$ reaction as compared with the experimental (symbols) and JENDL-4.0 (dashed line) data

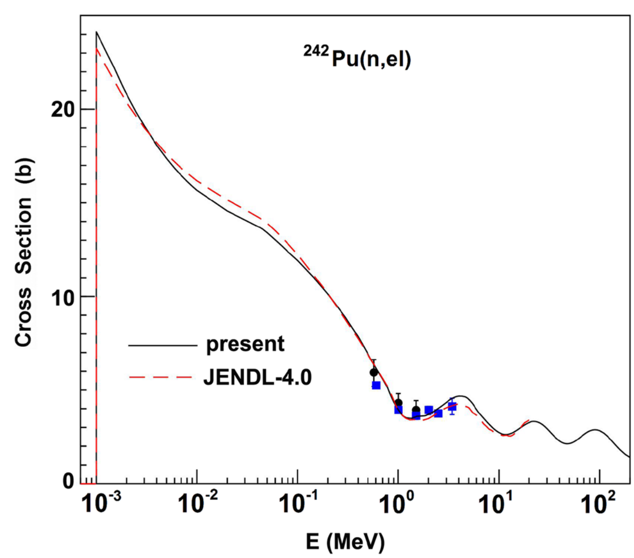

Fig. 13 (Color online) Same as Fig. 12, but for neutron elastic scattering cross section

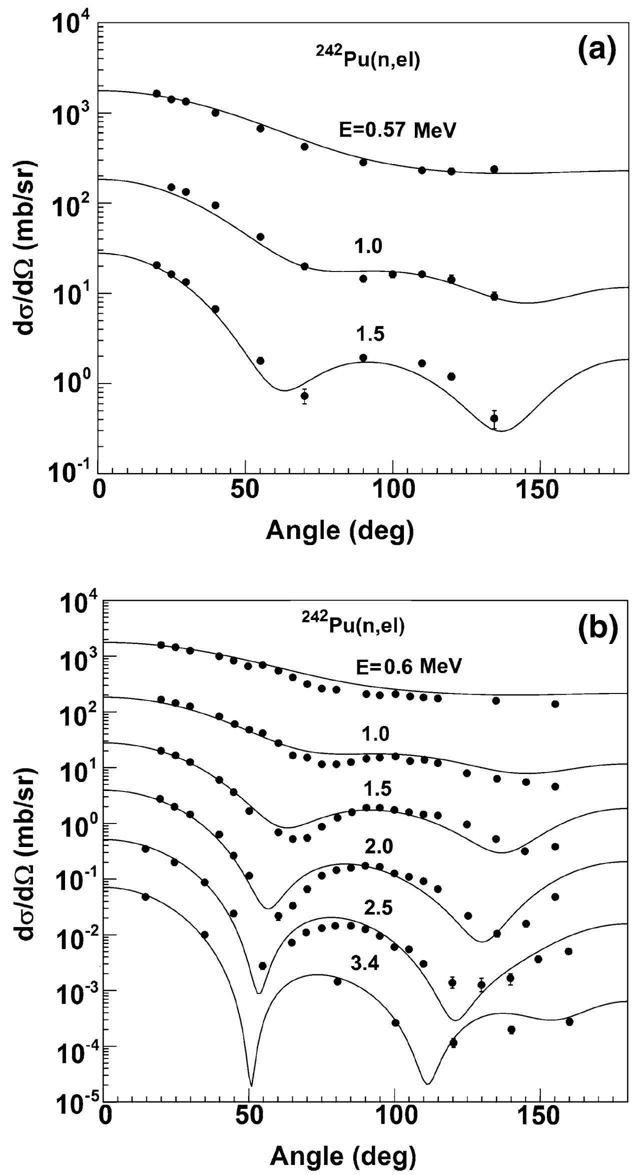

Fig. 14 Elastic scattering angular distributions for n + ^{242}Pu reaction. **a** The experimental data (symbols) are obtained from Ref. [43]. **b** The experimental data (symbols) are obtained from Ref. [44]. The data are shifted downward by factors of 10^0, 10^{-1}, 10^{-2}, etc

energy range of 1–4 MeV, as shown in Fig. 4. It should be noted that the two sets of experimental data contradict each other at incident energies greater than 1 MeV, where the experimental data on the elastic scattering cross section obtained from Ref. [27] are even greater than those obtained from Ref. [30], which comprise the contribution of not only the elastic scattering but also some inelastic scatterings.

Figures 5, 6, 7 and 8 show the comparisons of the calculated cross sections of the neutron inelastic scatterings to the 1st, 2nd, 5th, and 9th–11th excited states of ^{240}Pu with

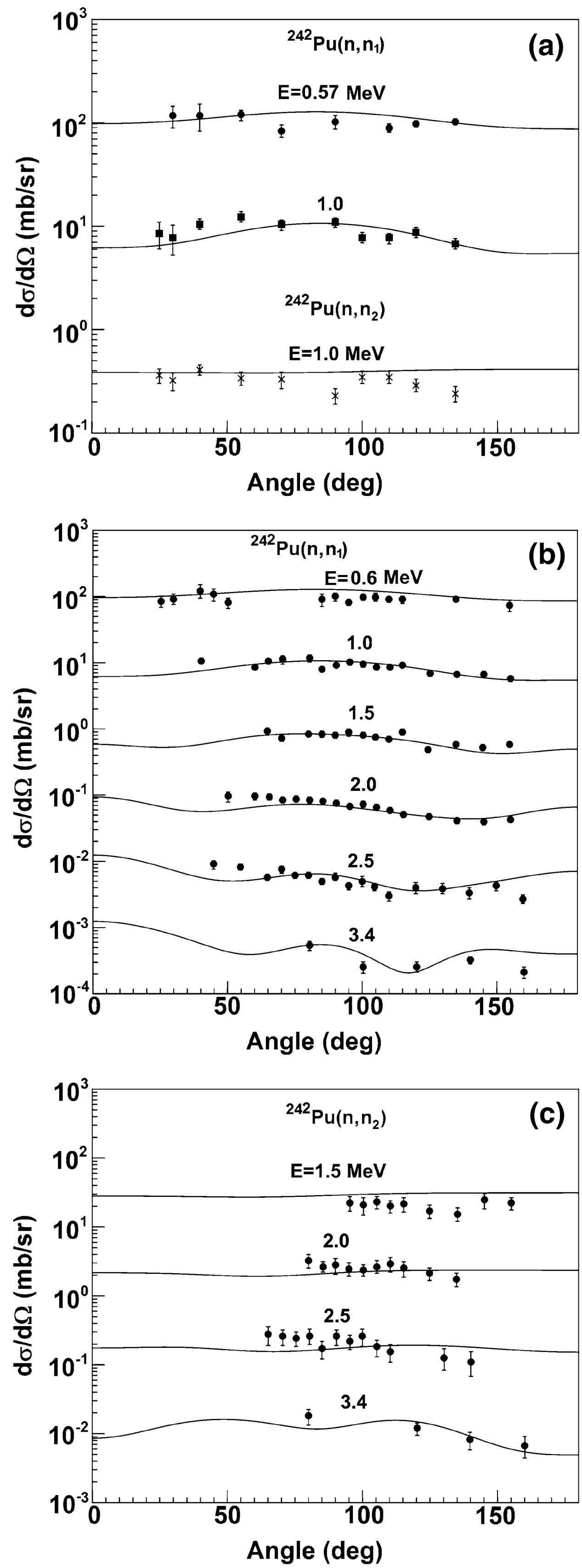

◀**Fig. 15 a** Calculated angular distributions of neutron inelastic scatterings to the first and second excited levels of ^{242}Pu (solid lines) as compared with the experimental data (symbols) obtained from Ref. [43]; **b** calculated angular distribution of the neutron inelastic scattering to the first excited level of ^{242}Pu (solid lines) as compared with the experimental data (symbols) obtained from Ref. [44]; **c** Calculated angular distribution of the neutron inelastic scattering to the second excited level of ^{242}Pu (solid lines) as compared with the experimental data (symbols) obtained from Ref. [44]. The data are shifted downward by factors of 10^{0}, 10^{-1}, 10^{-2}, etc

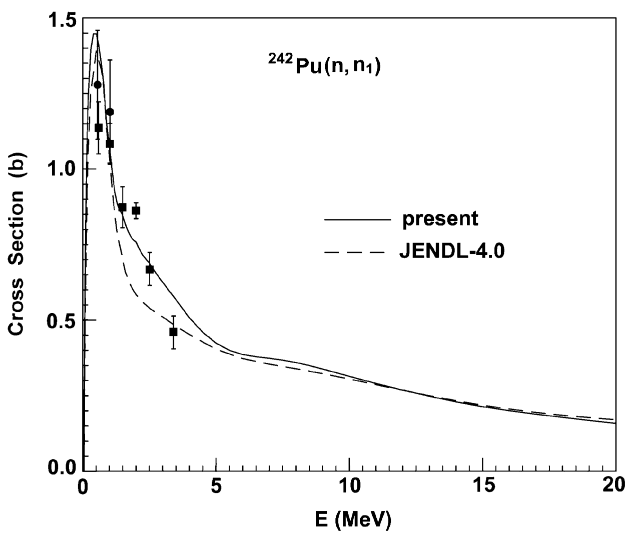

Fig. 16 Calculated cross section of neutron inelastic scattering to the first excited level of ^{242}Pu (solid line) as compared with the experimental (symbols) and JENDL-4.0 (dashed line) data

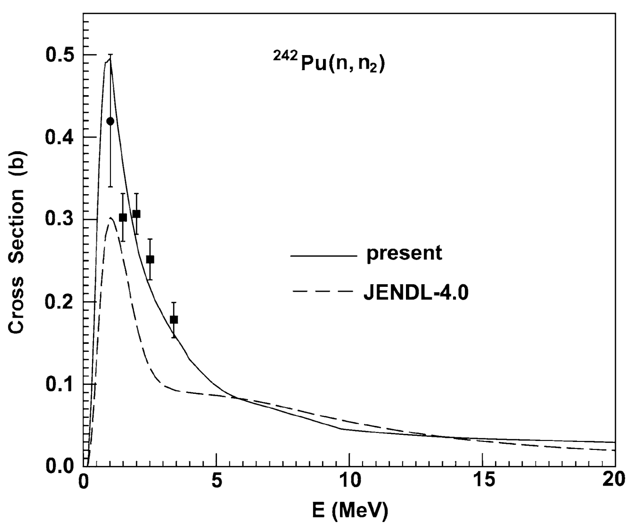

Fig. 17 Same as Fig. 16, but for neutron inelastic scattering to the second excited level of ^{242}Pu

experimental data [27], respectively. The calculated results are in reasonable agreement with the experimental data.

The calculated (n, γ) cross section is compared with the experimental data [31] presented in Fig. 9. The calculated result reproduces the experimental data well.

The comparison of the calculated fission cross section with the experimental data [32–36] for an incident energy less than 200.0 MeV is shown in Fig. 10. The present result is in good agreement with the recently obtained experimental data [32–34], and it is slightly greater than that of the ENDF/B-VII.1 and JENDL-4.0 data for incident energies less than 20 MeV, where the present result fits the recent experimental data obtained from Refs. [32, 33] better, while the ENDF/B-VII.1 and JENDL-4.0 data fit the experimental data obtained from Refs. [35, 36] better.

The number of neutrons per fission obtained using systematics is shown in Fig. 11. A good agreement with the experimental data [37–40] is observed.

3.2 n + ^{242}Pu reaction

The calculated total cross section is shown in Fig. 12. It can be observed that the calculated result reproduces the experimental data [41, 42] well and has some discrepancies with the data obtained from JENDL-4.0 at low energies.

Two sets of consistent experimental data regarding the cross sections and angular distributions of neutron elastic scattering and inelastic scatterings to the first and second excited levels of ^{242}Pu were presented by Drake et al. [43] and Haouat et al. [44], respectively. The present results reproduce the experimental data well, as shown in Figs. 13, 14, 15, 16 and 17, and are superior to the JENDL-4.0 data

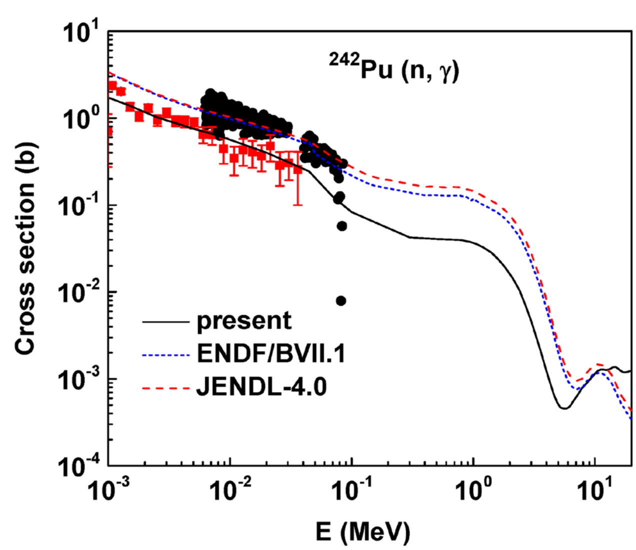

Fig. 18 (Color online) Calculated result of ^{242}Pu(n, γ) reaction cross section (solid line) as compared with the experimental (solid circles [45], solid squares [46]), ENDF/B-VII.1 (short-dashed line), and JENDL-4.0 (dashed line) data

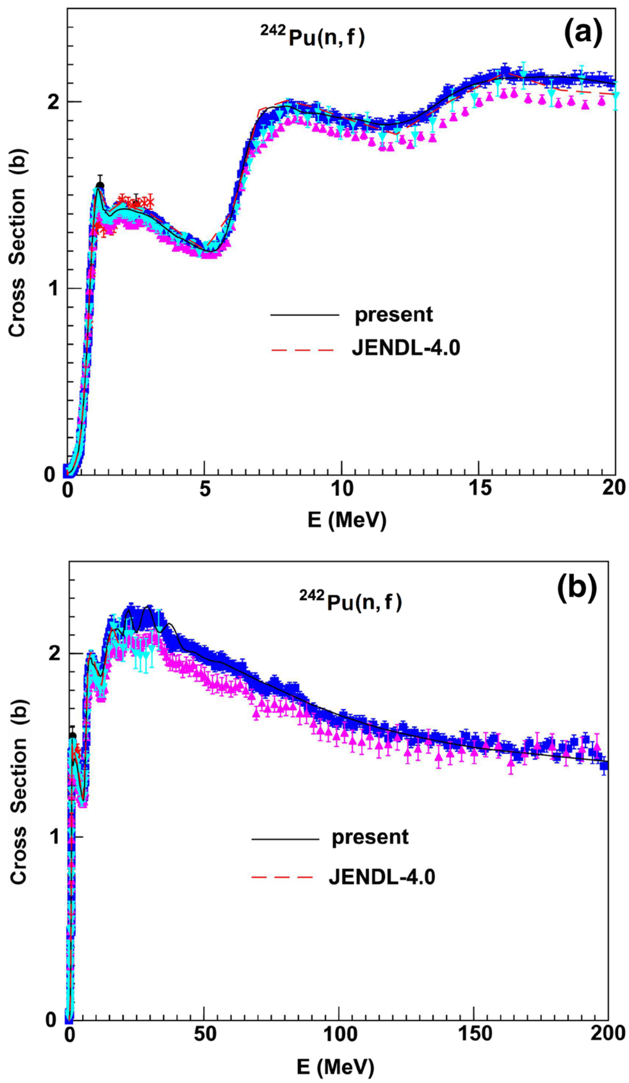

Fig. 19 (Color online) Calculated fission cross section (solid lines) for $n + {}^{242}$Pu reaction as compared with the experimental data (solid squares [32], lower triangles [35], upper triangles [36], crosses [47], solid circles [48]), and JENDL-4.0 data (dashed lines). **a** Incident energies less than 20 MeV and **b** Incident energies less than 200 MeV

in fitting the experimental data of the (n, n_2) reaction cross section.

Two sets of (n, γ) cross sections were measured by Hockenbury et al. [45] in 1975 and Buckner et al. [46] in 2016, respectively. The experimental data obtained from Ref. [45] are approximately three times greater than those obtained from Ref. [46], which were measured at LANSCE. These experimental data are compared with the present model calculation and the ENDF/B-VII.1 and JENDL-4.0 data in Fig. 18. It can be observed that the data from ENDF/B-VII.1 and JENDL-4.0 pass through the experimental data obtained from Ref. [45], while our result

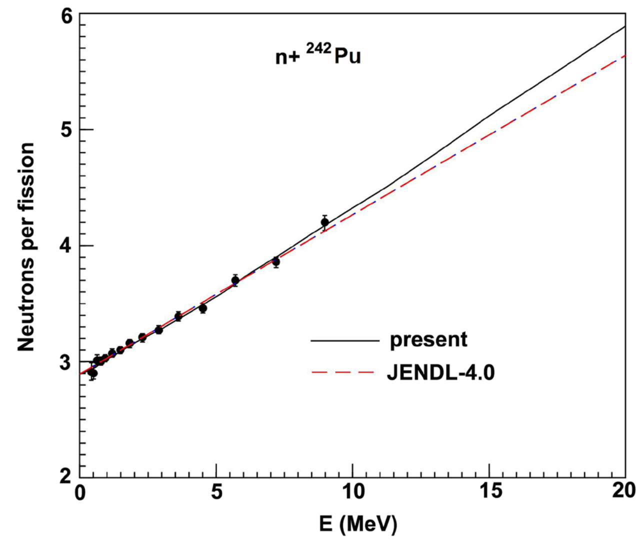

Fig. 20 (Color online) Calculated result of the number of neutrons per fission (solid line) for $n + {}^{242}$Pu reaction as compared with the experimental (symbols) and JENDL-4.0 (dashed line) data

is consistent with the new experimental data obtained from Ref. [46].

The comparison of the calculated fission cross section with the experimental data [32, 35, 36, 47, 48] for incident energies less than 200 MeV is shown in Fig. 19. The obtained result is in good agreement with the recent experimental data obtained from Refs. [32, 47, 48].

The number of neutrons per fission obtained using systematics is shown in Fig. 20. A good agreement with the experimental data [40] is observed.

3.3 $n + {}^{244}$Pu reaction

At present, experimental data [35, 36, 49–51] regarding fission cross section for an $n + {}^{244}$Pu reaction are limited. The calculated result is in good agreement with those obtained from Ref. [36] for incident energies less than 140 MeV but is less than those for incident energies less than 140 MeV, as shown in Fig. 21. A trend can be observed in Figs. 10, 19 and 21 that the fission cross sections decrease as the neutron number increases.

No experimental data are available regarding the cross sections of the total inelastic scattering, $(n, 2n)$, $(n, 3n)$ reactions, energy spectra, and energy-angle distributions of neutron and light-charged-particle emissions for $n + {}^{240,242,244}$Pu reactions. All these data are predicted by the theoretical models.

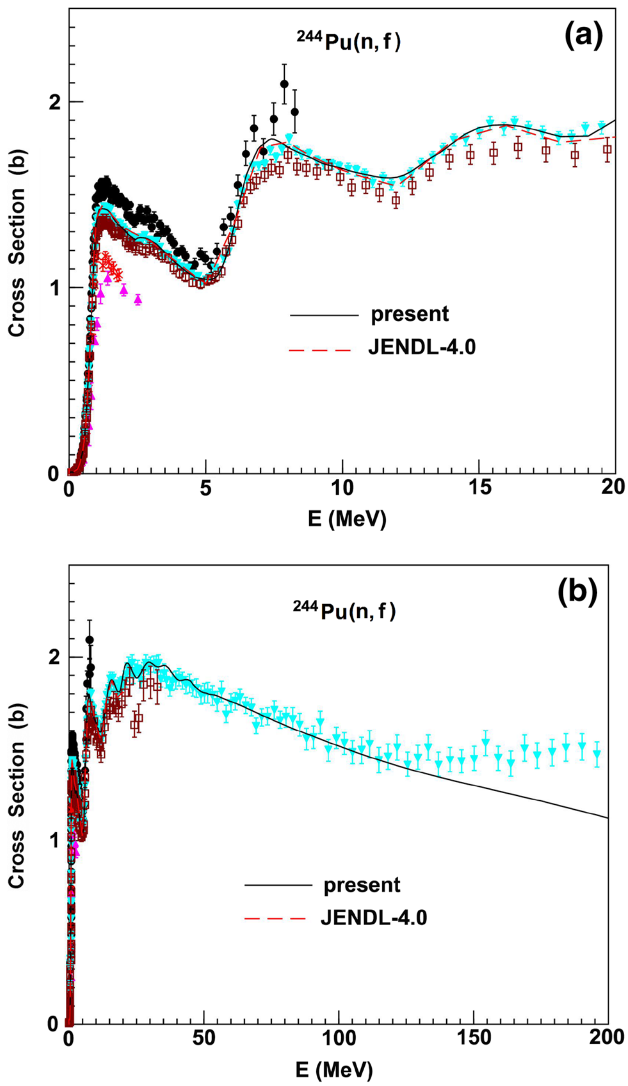

Fig. 21 (Color online) Calculated fission cross section (solid lines) for n + ^{244}Pu reaction as compared with the experimental data (squares [35], lower triangles [36], solid circles [49], crosses [50], upper triangles [51]), and JENDL-4.0 data(dashed lines). **a** Incident energies less than 20 MeV and **b** incident energies less than 200 MeV

4 Summary

All cross sections, angular distributions, energy spectra, and energy-angle distributions for neutron-induced reactions on ^{240}Pu, ^{242}Pu, and ^{244}Pu are consistently calculated using theoretical nuclear models at incident energies less than 200 MeV. The calculated results are generally in good agreement with the experimental data and reproduce them better than the evaluated data from ENDF/B-VII.1 and JENDL-4.0 for some reaction channels. The present results have been transformed into ENDF-B formatted data for the purpose of their application. The code for analyzing the covariances of the data is currently under development. The covariances will be given in the next step.

References

1. C.D. Bowman, E.D. Arthur, P.W. Lisowski et al., Nuclear energy generation and waste transmutation using an accelerator-driven intense thermal neutron source. Nucl. Instrum. Meth. Phys. Res. A **320**, 336–367 (1992). https://doi.org/10.1016/0168-9002(92)90795-6
2. A.J. Koning, J.-P. Delaroche, O. Bersillon, Nuclear data for accelerator driven systems: nuclear models, experiments and data libraries. Nucl. Instrum. Meth. Phys. Res. A **414**, 49–67 (1998). https://doi.org/10.1016/S0168-9002(98)00528-2
3. H. Guo, Y. Han, T. Ye et al., Theoretical analysis and evaluation for neutron-induced reaction on ^{239}Pu. Ann. Nucl. Energy **108**, 151–162 (2017). https://doi.org/10.1016/j.anucene.2017.04.043
4. K. Shibata, O. Iwamoto, T. Nakagawa et al., JENDL-4.0: a new library for nuclear science and engineering. J. Nucl. Sci. Technol. **48**, 1–30 (2011). https://doi.org/10.1080/18811248.2011.9711675
5. M.B. Chadwick, M. Herman, P. Oblozinsky et al., ENDF/B-VII.1 nuclear data for science and technology: cross sections, covariances, fission product yields and decay data. Nucl. Data Sheets **112**, 2887–2996 (2011). https://doi.org/10.1016/j.nds.2011.11.002
6. Y. Han, Y. Xu, H. Liang et al., Global phenomenological optical model potential of nucleon-actinide reaction for energies up to 300 MeV. Phys. Rev. C **81**, 024616 (2010). https://doi.org/10.1103/PhysRevC.81.024616
7. P.D. Kunz, *Distorted Wave Code DWUCK4* (University of Colorado, Denver, 1994)
8. J. Zhang, A unified Hauser-Feshbach and exciton model for calculating double-differential cross sections of neutron-induced reactions below 20 MeV. Nucl. Sci. Eng. **114**, 55–63 (1993). https://doi.org/10.13182/NSE93-3
9. W. Dilg, W. Schantl, H. Vonach, Level density parameters for the back-shifted fermi gas model in the mass range $40 < A < 250$. Nucl. Phys. A **217**, 269–298 (1973). https://doi.org/10.1016/0375-9474(73)90196-6
10. A. Iwamoto, K. Harada, Mechanism of cluster emission in nucleon-induced preequilibrium reactions. Phys. Rev. C **26**, 1821–1834 (1982). https://doi.org/10.1103/PhysRevC.26.1821
11. J. Zhang, S. Yan, C. Wang, The pick-up mechanism in composite particle emission processes. Z. Phys. A **344**, 251–258 (1992). https://doi.org/10.1007/BF01303018
12. A.V. Ignatyuk, G.N. Smirenkin, A.S. Tishin, Phenomenological description of the energy dependence of the level density parameter. Sov. J. Nucl. Phys. **21**, 255 (1975)
13. Q. Shen et al., Monte-Carlo calculations of nucleon emitted and energy deposition in cylindrical targets induced by intermediate energy protons, in *The 2nd international conference on accelerator-driven transmutation technologies and applications*, Kalmar, Sweden (1997) p. 686
14. C. Kalbach, F.M. Mann, Phenomenology of continuum angular distributions. I. Systematics and parametrization. Phys. Rev. C **23**, 112–123 (1981). https://doi.org/10.1103/PhysRevC.23.112
15. C. Kalbach, Systematics of continuum angular distributions: Extensions to higher energies. Phys. Rev. C **37**, 2350–2370 (1988). https://doi.org/10.1103/PhysRevC.37.2350
16. J. Zhang, UNF code for fast neutron reaction data calculations. Nucl. Sci. Eng. **142**, 207–219 (2002). https://doi.org/10.13182/NSE02-02
17. C. Cai, MEND: a program for calculating the complete set of nuclear data of medium-heavy nuclei in a medium-low energy region. Nucl. Sci. Eng. **153**, 93 (2006). https://doi.org/10.13182/NSE05-06CCA

18. Z. Wu, H. Liang, Y. Han, Theoretical calculations and evaluations of n+^{23}Na reaction. Nucl. Sci. Tech. **27**, 102 (2016). https://doi.org/10.1007/s41365-016-0092-8
19. Y. Han, Y. Shi, Q. Shen, Deuteron global optical model potential for energies up to 200 MeV. Phys. Rev. C **74**, 044615 (2006). https://doi.org/10.1103/PhysRevC.74.044615
20. Y. Xu, H. Guo, Y. Han et al., Applicability of the systematic helium-3 potential for triton-nucleus reactions. Int. J. Mod. Phys. E **24**, 1550005 (2015). https://doi.org/10.1142/S0218301315500056
21. Y. Xu, H. Guo, Y. Han et al., Helium-3 global optical model potential with energies below 250 MeV. Sci. China Phys. Mech. Astron. **54**, 2005 (2011). https://doi.org/10.1007/s11433-011-4488-5
22. X. Su, Y. Han, Global optical model potential for alpha projectile. Int. J. Mod. Phys. E **24**, 1550092 (2015). https://doi.org/10.1142/S0218301315500925
23. A. Gilbert, A.G.W. Cameron, A composite nuclear-level density formula with shell corrections. Can. J. Phys. **43**, 1446–1496 (1965). https://doi.org/10.1139/p65-139
24. N. Bohr, J.A. Wheeler, The mechanism of nuclear fission. Phys. Rev. **56**, 426–450 (1939). https://doi.org/10.1103/PhysRev.56.426
25. D.L. Hill, J.A. Wheeler, Nuclear constitution and the interpretation of fission phenomena. Phys. Rev. **89**, 1102–1145 (1953). https://doi.org/10.1103/PhysRev.89.1102
26. D.G. Madland, J.R. Nix, New calculation of prompt fission neutron spectra and average prompt neutron multiplicities. Nucl. Sci. Eng. **81**, 213–271 (1982). https://doi.org/10.13182/NSE82-5
27. A.B. Smith, J.F. Whalen, P. Lambropoulos, Fast neutron total and scattering cross sections of plutonium-240. Nucl. Sci. Eng. **47**, 19–28 (1972). https://doi.org/10.13182/NSE72-A28417
28. W.P. Poenitz, J.F. Whalen, A.B. Smith, Total neutron cross sections of heavy nuclei. Nucl. Sci. Eng. **78**, 333–341 (1981). https://doi.org/10.13182/NSE81-A21367
29. W. P. Poenitz, J. F. Whalen, Neutron total cross section measurements in the energy region from 47 keV to 20 MeV. ANL-NDM-80 (1983)
30. A. B. Smith, P. T. Guenther, On neutron inelastic-scattering cross sections of ^{232}Th, ^{233}U, ^{235}U, ^{238}U, ^{239}Pu and ^{240}Pu. ANL-NDM-63 (1982)
31. R.W. Hockenbury, W.R. Moyer, R.C. Block, Neutron Capture, Fission, and Total Cross Sections of ^{240}Pu from 20 eV to 30 keV. Nucl. Sci. Eng. **49**, 153–161 (1972). https://doi.org/10.13182/NSE72-A35503
32. F. Tovesson, T.S. Hill, M. Mocko et al., Neutron induced fission of ^{240,242}Pu from 1 eV to 200 MeV. Phys. Rev. C **79**, 014613 (2009). https://doi.org/10.1103/PhysRevC.79.014613
33. A.B. Laptev, AYu. Donets, V.N. Dushin et al., Neutron-induced fission cross sections of ^{240}Pu, ^{243}Am, and ^{Nat}W in the energy range 1–200 MeV, in *Proceedings of International Conference Nuclear Data for Science and Technology*, Santa Fe (2004), pp. 865–869
34. A. V. Fomichev, V.N. Dushin, S.M. Soloviev et al., Neutron induced fission cross sections For ^{240}Pu, ^{243}Am, ^{209}Bi, ^{nat}W measured relative to ^{235}U in the energy range 1-350 MeV. RI-262 (2004)
35. J.W. Behrens, R.S. Newbury, J.W. Magana, Measurements of the neutron-induced fission cross sections of ^{240}Pu, ^{242}Pu, and ^{244}Pu relative to ^{235}U from 0.1 to 30 MeV. Nucl. Sci. Eng. **66**, 433–441 (1978). https://doi.org/10.13182/NSE78-A27227
36. P. Staples, K. Morley, Neutron-induced fission cross section ratios for ^{239}Pu, ^{240}Pu, ^{242}Pu, and ^{244}Pu Relative to ^{235}U from 0.5 to 400 MeV. Nucl. Sci. Eng. **129**, 149–163 (1998). https://doi.org/10.13182/NSE98-A1969
37. M. V. Savin, Yu.A. Khokhlov, Yu.S. Zamjatnin et al., The average number of prompt neutrons in fast neutron induced fission of ^{235}U, ^{239}Pu and ^{240}Pu, in *Nuclear Data for Reactors Conference*, 2, Helsinki (1970), p. 157
38. J. Frehaut, G. Mosinski, R. Bois et al., Measurement of the average number, nu-bar, of the prompt neutrons emitted in the ^{240}Pu and ^{241}Pu fission induced by neutrons of energy between 1.5 and 15 MeV. CEA-R-4626 (1974)
39. V. G. Vorobeva, N.P. Dyachenko, B.D. Kuzminov et al., Determination of energy dependence of NU for uranium-238, plutonium-240 and plutonium-241 from an analysis of the fission energy balance. YK-15, 3 (1974)
40. Yu. A. Khokhlov, I.A. Ivanin, V.I. Inkov et al., Measurement results of average neutron multiplicity from neutron induced fission of actinides in 0.5–10 MeV energy range, in *Proceedings of International Conference Nuclear Data for Science and Technology*, Gatlinburg (1994), p. 272
41. T.E. Young, S.D. Reeder, Total neutron cross section of ^{242}Pu. Nucl. Sci. Eng. **40**, 389–395 (1970). https://doi.org/10.13182/NSE70-A20190
42. M. S. Moore, P.W. Lisowski, G.L. Morgan et al., Total cross section of ^{242}Pu between 0.7 and 170 MeV. in *Conference on Nuclear Cross Sections for Technology*, Knoxville (1979), p. 703
43. D. M. Drake, M. Drosg, P. Lisowski, et al., Neutron scattering cross sections for Pu-242. LA-7855 (1979)
44. G. Haouat, J. Lachkar, C.H. Lagrange et al., Neutron scattering cross sections for ^{232}Th, ^{233}U, ^{235}U, ^{238}U, ^{239}Pu and ^{242}Pu between 0.6 and 3.4 MeV. Nucl. Sci. Eng. **81**, 491–511 (1982). https://doi.org/10.13182/NSE82-A21439
45. R. W. Hockenbury, A. J. Sanislo, N. N. Kaushal, keV capture cross section of ^{242}Pu, in *Conference on Nuclear Cross Sections and Technology*, 2, Washington (1975), p. 584
46. M.Q. Buckner, C.Y. Wu, R.A. Henderson et al., Absolute measurement of the ^{242}Pu neutron-capture cross section. Phys. Rev. C **93**, 044613 (2016). https://doi.org/10.1103/PhysRevC.93.044613
47. P. Salvador-Castineira, T. Brys, R. Eykens et al., Neutron induced fission cross sections of ^{242}Pu from 0.3 MeV to 3 MeV. Phys. Rev. C **92**, 044606 (2015). https://doi.org/10.1103/PhysRevC.92.044606
48. C. Matei, F. Belloni, J. Heyse et al., Absolute cross section measurements of neutron-induced fission of ^{242}Pu from 1 to 2.5 MeV. Phys. Rev. C **95**, 024606 (2017). https://doi.org/10.1103/PhysRevC.95.024606
49. M.S. Moore, J.A. Wartena, H. Weigmann et al., Neutron induced fission cross section of ^{244}Pu. Nucl. Phys. A **393**, 1–14 (1983). https://doi.org/10.1016/0375-9474(83)90061-1
50. B. M. Gokhberg, S. M. Dubrovina, V. A. Shigin, Fast neutron fission cross-section of ^{244}Pu. YFI-22, 10 (1976)
51. E. F. Fomushkin, B.K. Maslennikov, G.F. Novoselov et al., Fission Threshold Measurement of ^{244}Pu by Neutrons. YFI-22, 11 (1976)